Biuletyn WAT
Vol. LXVIII, Nr 3, 2019

A method for the approximate determination of microparticle amount and mass in biological mixtures using a fractionation process in a centrifugal force field

ANDRZEJ GÓRKA

Military University of Technology, Institute of Optoelectronics,
2 Gen. S. Kaliskiego Str., 00-908 Warsaw, Poland, gorka@upcpoczta.pl

Abstract. The paper presents a simplified method of estimating the amount and specific mass of microparticles in complex biological mixtures using the fractionation process in the field of centrifugal forces. In the presented method, using the heaviest blood cells – erythrocytes – as an example, a geometric model of a binary fraction in a borderline equilibrium state formed in the process of blood fractionation was used. In this model, an approximated shape of the erythrocyte and a sample normal distribution of the size and number of microparticles in the examined model fraction filled with erythrocytes were used. Based on publicly available blood data, it has been shown that it is possible to estimate the amount and specific weight of microparticles. The accuracy of such estimation generally depends on the precision of representation of shapes, the degree of filling the fraction with microparticles and on the individual quantitative and dimensional distribution of these particles in the examined fraction. The above conclusions, which determine the accuracy of the method presented, were verified in the paper with the use of rheological blood data, commonly available in literature for various types of measuring containers, which affect the level of filling of a given fraction with microparticles.
Keywords: fractionation of biological mixtures, fractionation of blood components, erythrocyte model, erythrocyte shape, blood components
DOI: 10.5604/01.3001.0013.5552

1. Background

In medical examinations, peripheral blood morphology is the basic source of information about the patient's health. It principally concerns a quantitative assay of the morphotic components of blood. As liquid tissue, blood is also used

to acquire blood concentrates for treatment [1-6], therapeutic cosmetology and apheresis procedures [7-9]. In standard examination schemes, blood is taken using a conventional donation method. In the case of apheresis, however, the procedure may be applied to the entire volume of blood, provided that blood losses are made up for by a healthy fraction or by morphologically compatible replacement fluids. In laboratory morphology tests and in apheresis procedures, rotational blood fractionation in a centrifugal force field is used. The basic aim of such a process is the selective enrichment or separation of specific blood fractions for therapy or medical prevention purposes. In many cases, it is a multi-phase process, often performed in continuous or batch mode. These assays are work-intensive and difficult to analyse without sufficient research facilities.

2. Introduction

Most regular morphological blood tests are based on approximate assessment methods of the quantitative and qualitative properties of the morphotic components of blood [10-17]. Due to the small amounts of blood taken for analysis, averaged values of the measured parameters are used, compared in each instance with statistical values. In such cases, techniques that are methodologically strongly connected to specific measurement instruments are applied. The results of such tests in many cases are not comparable. The greatest inconsistencies in such assays concern the estimation of individual morphotic component quantities. In practice, due to the small amounts of blood taken for testing and the accuracy of the separation methods used, quantitative assays always carry a degree of measurement error. Minimisation of such errors can most readily be achieved by individual and population-level standardisation of peripheral blood components and by dynamic development of new methods of biochemical blood cell activation [3, 18, 19]. The expectations above necessitate further expanded studies on filtration [20, 21] and fractioning of complex biological mixtures in a centrifugal force field [22]. This paper concerns the theoretical aspects of the fractionation process of complex biological mixtures exemplified by peripheral blood. Blood is defined as a biologically stable mixture of morphotic microparticles (blood cells) in a matrix of uniform plasma as the base solution. It is assumed that thermally and biochemically stable microparticles do not undergo aggregation or coagulation, and do not degrade throughout the volume of the test mixture. It is further believed that analysis of the microparticle fractionation process only concerns a boundary state where no migration of microparticles in the base fluid (plasma) occurs [22]. A diagram of the borderline state of individual fractions, formed through the process of fractionation in a centrifugal force field, is provided in Fig. 1.

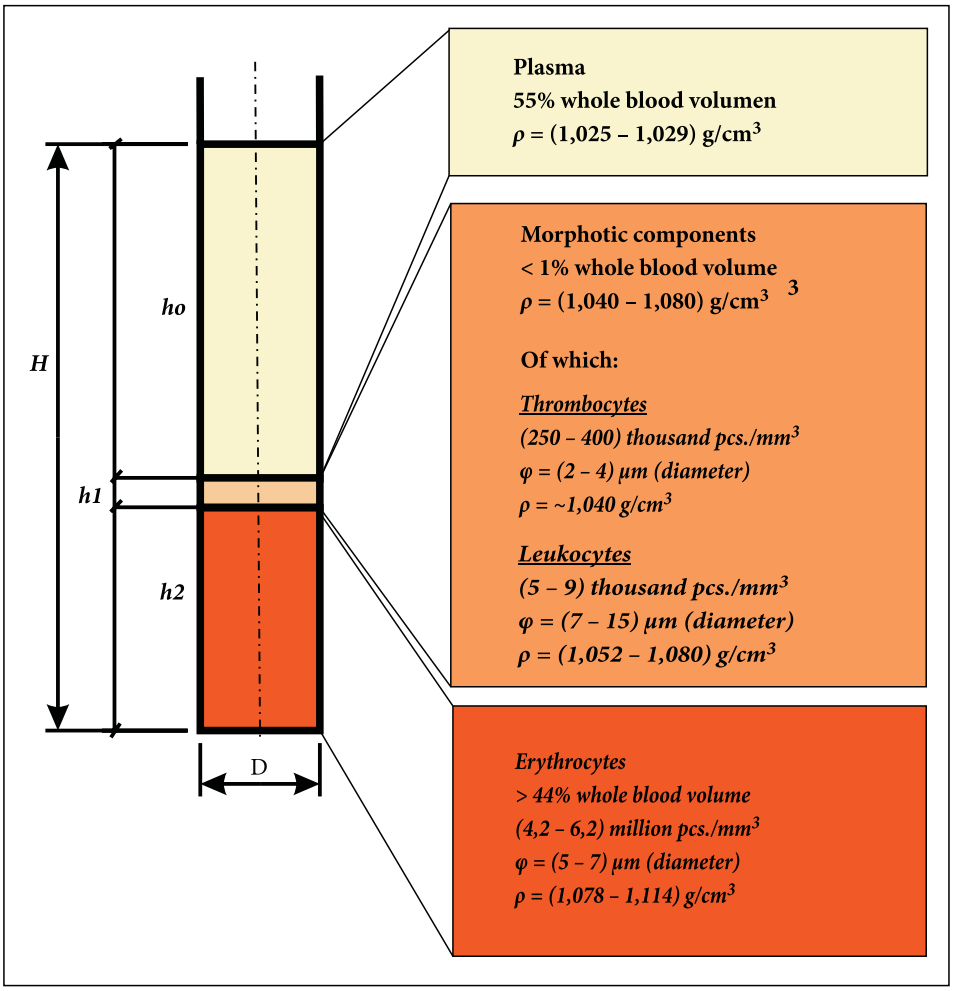

Fig. 1. A sample of peripheral blood with a mass density of ρ = (1.053-1.057) g/cm^3 after the fractionation process in a centrifugal force field — on the following of publications [23-26]

Based on data from papers [23-26], the separation boundaries of individual fractions in the boundary equilibrium state, as shown in Fig. 1, will not be clearly defined. For this reason various means of improving this situation are used to increase practical separation accuracy of individual fractions [3, 26]. For example, the accuracy of determining fraction separation boundary positions can be greatly improved if complex fractioning procedures are used, e.g. ones employing buffers or mass separators. In this paper, due to its theoretical nature, attention was primarily focused on presenting a method for assessing the quantity and mass density of microparticles in biological samples using direct mixture fractioning in a centrifugal force

field. On account of the above, commonly available averaged data on peripheral blood [23-26] were used in the study. At the same time it was assumed that:

- microparticles do not undergo degradation, coagulation or deformation during the fractionation process,
- microparticles in mixtures are biochemically inactive and do not interact with one another,
- microparticle shape does not affect the fractionation process in a centrifugal force field,
- the effects of the gravity field on the fractionation process is negligible,
- in the centrifugal fractionation process, microparticle migration depends on: microparticle mass, centrifugal force, and buoyant force [22],
- once microparticle migration terminates, the fractionation process in a centrifugal force field creates a boundary state of stable equilibrium between the isolated fractions,
- in the boundary equilibrium state, the fractions are binary (a specific microparticle type in a base fluid matrix) and do not contain microparticles from other fractions.

The boundary equilibrium of the fractions formed in the centrifugal fractionation process constitutes the starting point in the discussed method of estimating the quantity and approximate mass of microparticles in the analysed fraction. According to the assumptions above, the accuracy of determining fraction separation boundary positions markedly affects the accuracy of estimating microparticle quantities in individual fractions. On the other hand, the accuracy of microparticle shape representation and quantitative distribution in a given fraction will decide how accurate their mass estimation is. Due to the simplified manner in which the method employed is presented in the paper, an approximate model of the microparticle shape (Fig. 2) and a standard normal distribution of microparticle size and quantity in the fraction analysed (erythrocytes — Fig. 1) were used in this analysis of microparticle quantity and mass density estimation. In laboratory practice, the accuracy of determining fraction separation boundary positions and individual size distribution will decide the accuracy and diagnostic characteristics of the method discussed. Consequently, calibrated measurement containers and methodologically comprehensive and accurate microscopic assays of size distribution and quantity of the studied microparticles in a given fraction should be used in such tests. Due to the theoretical nature of this paper, only commonly available data on peripheral blood were used for verification of the method discussed, while calculation examples were compared to a binary fraction of erythrocytes [22].

3. Geometric model of a binary fraction formed in a centrifugal force field

In the fractionation process, the heaviest and most numerous blood cells — erythrocytes — are deposited in the bottommost fraction (Fig. 1). This fraction is fairly uniform, with a high level of filling and minimal "contamination" by other microparticles. In this paper, it is considered a binary fraction formed of erythrocytes and uniform plasma as the fraction base fluid. If the shape and quantitative and size distribution of erythrocytes in a given fraction is known, knowing the mass densities of the entire fraction and of the base fluid [22] enables the estimation of the quantity and mass density of erythrocytes in this fraction. In literature, erythrocyte shape in 3D space is modelled based on various measurement methods [27-30]. It is often approximated using the Cassini oval [34-36]. The accuracy of this representation depends on the precision of determining the positions of foci points oval the Cassini, which is not excessively easy with typical optical microscopy. As a result, we have developed our own geometric model of the erythrocyte, which can easily be described using standard light microscopy. This model is based on a torus, as shown in Figure 2.

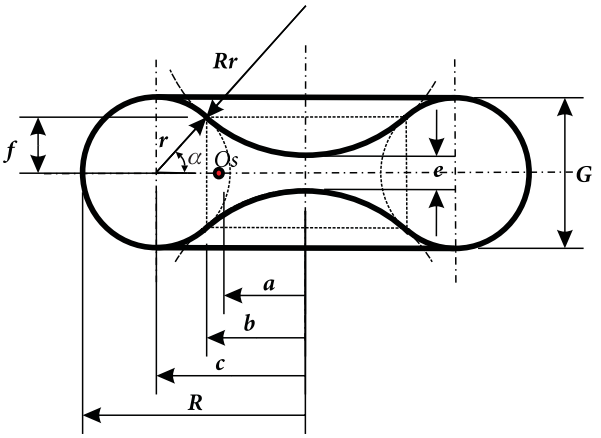

Fig. 2. Geometric model of the erythrocyte. Description of symbols in the text

The basic parameters of the above model are: torus radius *R*, torus thickness *G* and constriction values *e*. In microscopic observations of any erythrocyte, determination of the torus radius *R* and thickness *G* should pose no difficulty. Determining the precise constriction value *e* is not as easy. For healthy cells, this parameter is usually within the range (0.8-2.5) μm [25, 30, 33]. In the proposed model, constriction value *e* does not significantly affect the total volume of an erythrocyte and it is assumed that the value is correlated with cell thickness *G*. As a result, based

on the single cell volume geometric model shown in Figure 2, single cell volume V_e can be determined using equation (1):

$$V_e = V_t - V_{pw} + V_w - V_{cz}, \tag{1}$$

where: V_t — torus volume,
V_{pw} — volume of concave ring of revolution,
V_{cz} — volume of two spherical caps,
V_w — volume of central cylinder of revolution.

In equation (1), the volume of the model constituent solids are described by the following equations (symbols as in Figure 2):

- base torus volume V_t is defined by equation (2):

$$V_t = 2 \cdot \pi^2 \cdot c \cdot r^2, \tag{2}$$

where: $r = \dfrac{G}{2}$

$c = R - r$

- volume of central cylinder of revolution V_w is defined by equation (3):

$$V_w = 2 \cdot \pi \cdot b^2 \cdot f \tag{3}$$

where: $b = c - \sqrt{r^2 - f^2}$

$$f = r \cdot \frac{R_r + \dfrac{e}{2}}{R_r + r}$$

$$R_r = \frac{c^2 - r^2 + \dfrac{e^2}{4}}{2 \cdot r - e}$$

- volume of two spherical caps V_{cz} is defined by equation (4):

$$V_{cz} = \frac{\pi \cdot \left(f - \dfrac{e}{2} \right)}{3} \cdot \left[3 \cdot b^2 + \left(f - \frac{e}{2} \right)^2 \right] \tag{4}$$

- volume of concave ring of revolution V_{pw}, determined using the Pappus-Guldinus theorem [31], which takes into account the centre of gravity *Os* of a circle section at distance *a* from its centre (Fig. 2) is defined by equation (5):

$$V_{pw} = 2 \cdot \pi \cdot a \cdot S_p, \tag{5}$$

where: $a = R - r - \sqrt{r^2 - \frac{f^2}{4}}$

$$S_p = \pi \cdot r^2 \cdot \left[\frac{\arcsin(\alpha)}{360}\right] - \frac{r \cdot f}{2}$$

$$\alpha = \arcsin\left(\frac{f}{r}\right)$$

Under actual conditions, blood flow may contain erythrocyte cells at different stages of development, i.e. of different dimensions, mainly *R* and *G*. Standard laboratory methods of microscopic blood examinations [32-34] can be used to determine precise erythrocyte size distributions in the analysed blood samples in specific cases. Due to the scope and purpose of this paper, discussion is limited to a standard deviation of erythrocyte size in the analysed blood sample, assumed a priori. Due to the simplification adopted, erythrocyte size in the presented analysis is characterised by microparticle radius *R*, while dimensions *G* and *e* shall be functions of this radius. Furthermore, it was assumed that after the process of fractionating a given blood volume, in the boundary fraction equilibrium state, cells are arranged "losslessly", as illustrated in Fig. 3.

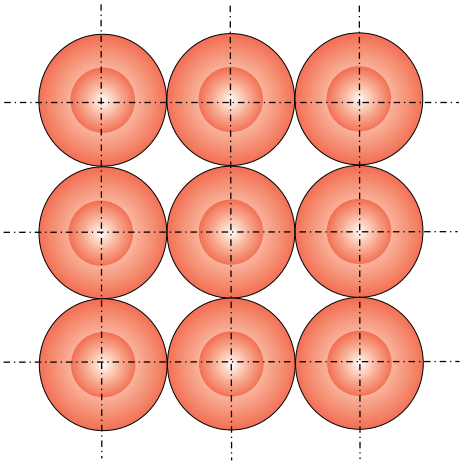

Fig. 3. Diagram of a cell arrangement under boundary equilibrium of the erythrocyte fraction, in the plane of the measurement container base

On this basis, the total number of cells in a single layer of the erythrocyte fraction, depending on the measurement container used, is defined by equations (6÷8):

— for containers with a square base, the amount of erythrocytes in a single layer n_{kw} is defined by equation (6):

$$n_{kw} = \left(\frac{a_{kw}}{2 \cdot R} \right)^2, \tag{6}$$

where: a_{kw} — dimension of measurement container base side;

— for containers with a base the shape of a hexagon inscribed in a circle with radius R_{ko} and with cells arranged as in Fig. 4, the amount of erythrocytes in a single layer n_{sz} is defined by equation (7):

$$n_{sz} = 1 + 6 \cdot \sum_{i=0}^{i=N} (i), \tag{7}$$

where: $N = \text{int}\left(\frac{\frac{R_{kw}}{R} - 1}{2} \right)$;

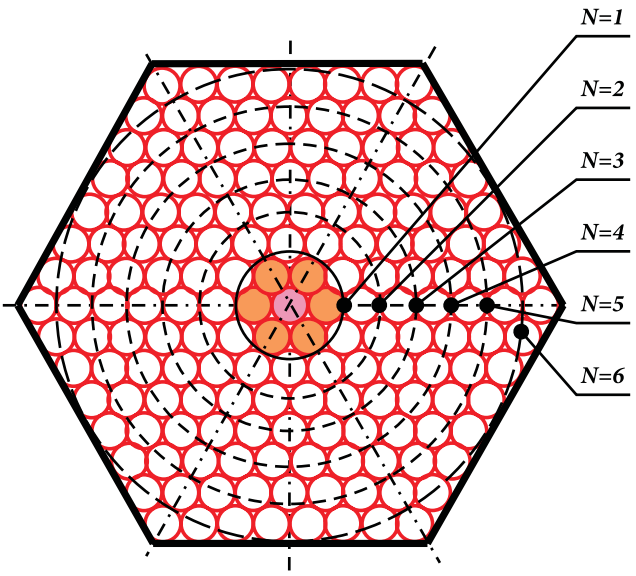

Fig. 4. Cell arrangement in a single layer of a regular hexagonal base container

— for cylindrical measurement containers with radius R_{ko} and with cells arranged as in Fig. 5, the amount of erythrocytes in a single layer n_{ko} is defined by equation (8):

$$n_{ko} = 1 + 6 \cdot \left\{ \sum_{i=0}^{i=N-1} (i) + \sum_{i=0}^{i=j} (N - 4 \cdot i) \right\}, \tag{8}$$

where: $N = \text{int}\left(\frac{\frac{R_{ko}}{R} - 1}{2} \right)$

$$j = \text{int}\left[\frac{(2-\sqrt{3}) \cdot (2 \cdot N + 1)}{4} \right]$$

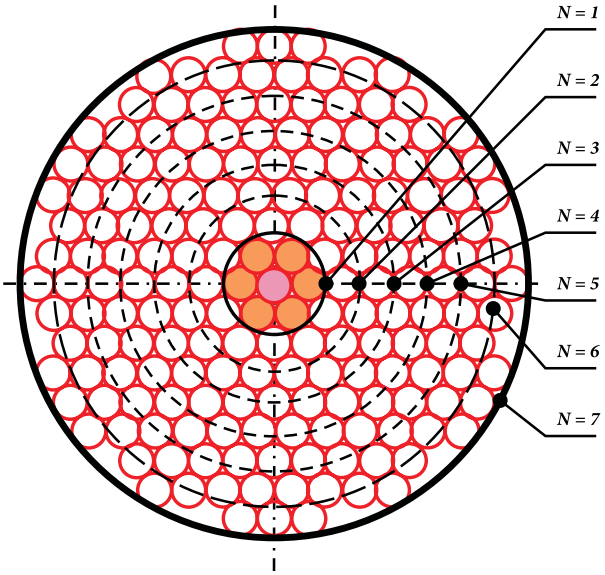

Fig. 5. Cell arrangement in a single layer of a cylindrical measurement container

In case of a known number of cells in a single layer of a measuring container and a known number of layers in the tested fraction (Fig. 1), we can estimate the average number of cells in this fraction, on the basis of equation (9):

$$n_{sr} = \frac{h_2}{G_{sr}} \cdot n, \tag{9}$$

where: h_2 — fraction height (Fig. 1),
G_{sr} — mean erythrocyte thickness in a given fraction (Fig. 2),
n — number of cells in a single layer, depending on the shape of the measurement container base.

Mean number of cells n_{sr} (9) with mean volume V_e (1) in a given fraction can only be used for preliminary assessment of both the level of filling and mass density of the microparticles filling the fraction. When estimating fraction filling levels and microparticle mass density in more accurate tests, the microparticle size distribution specific to the fraction must always be considered. This distribution, determined on the basis of detailed microscopic examinations of erythrocyte fractions with height h_2 (Fig. 1), and the estimated microparticle amount in the fraction formed, determine the description accuracy in the presented fraction model. If the total mass densities of the binary fraction and of the base fluid are known [22], it is possible to estimate the mass density of the microparticles themselves that fill the analysed fraction, and their mass.

4. Method of estimating microparticle mass density using a geometric fraction model

In laboratory practice, blood for testing is usually drawn into cylindrical containers that can be used directly for fractionation, both in the gravity field and in a centrifugal force field. In the case of the presented method of estimating microparticle mass density made using the geometric fraction model, the filling level that takes into account the actual microparticle size distribution $\mathbf{s_w}$ are defined by equation (10):

$$s_w = \frac{V_{ce}}{V_f}, \tag{10}$$

where: V_{ce} — total volume of microparticles of different sizes in the analysed fraction;
$V_f = F_p \cdot h_2$ — volume of fraction with height h_2 (Fig. 1);
F_p — surface area of the measurement container base.

In equation (10), the total volume of microparticles V_{ce}, which are greatly varied in terms of size and quantity in a given fraction, can only be determined based on microscopic statistical tests. The primary purpose of such tests is also to determine the individual distribution of the amount and size of these microparticles in the fraction. Due to the theoretical nature and narrower thematic scope and purpose of this paper, which is only a presentation of an estimation of the quantity and mass density of the microparticles filling a given fraction, the paper analyses only the normal distribution of microparticle size in the analysed erythrocyte fraction, using a cylindrical measurement container (Fig. 1). It is assumed in the analysis presented that the size of erythrocyte constriction ***e*** and thickness ***G*** are correlated with its diameter as described by equation 11:

$$G_i = \frac{2 \cdot R_i}{4};\ e_i = \frac{G_i}{2}, \tag{11}$$

where: R_i — current microparticle radius.

In this account, the actual multi-dimensional distribution of erythrocyte size was simplified to a standard one-dimensional distribution according to radius *R*.

For a symmetrical normal distribution of microparticle size in the analysed fraction, and considering the 3σ principle, individual layers and their shares are summarised in Table no. 1.

Table 1

Schematic diagram of the designation of layers and their shares in the case of symmetrical normal distribution of micro-particles in a given fraction

Current microparticle radius R_i	Correlated current microparticle thickness G_i	Current microparticle volume V_{ei}	Microparticle share in a given fraction P_i [%]
R_1	G_1	V_{e1}	$P_1 = 0.1$
R_2	G_2	V_{e2}	$P_2 = 2.1$
R_3	G_3	V_{e3}	$P_3 = 13.6$
R_4	G_4	V_{e4}	$P_4 = 34.2$
R_5	G_5	V_{e5}	$P_5 = 34.2$
R_6	G_6	V_{e6}	$P_6 = 13.6$
R_7	G_7	V_{e7}	$P_7 = 2.1$
R_8	G_8	V_{e8}	$P_8 = 0.1$
$R_{sr} = \frac{R_8 + \cdots + R_1}{8}$	$G_{sr} = \frac{G_8 + \cdots + G_1}{8}$	$V_{esr} = \frac{V_{e8} + \cdots + V_{e1}}{8}$	$P = 100$

Due to the principle of completely filling individual layers with microparticles, and considering the predicted estimation error for a given distribution, the sum of all layer heights h_s should be lower than the actual height h_2 of the analysed fraction. To minimise the above error, the difference can be filled by the mean value or median of microparticle size R_{sr} from the entire population. The error correction method shown above improves the accuracy of the discussed method of estimating the quantity and mass density of microparticles filling a given fraction, particularly when individual microparticle size distributions are used. According to the assumptions above, the number of microparticle layers in a given fraction with averaged shape parameters w_k is defined by equation (12):

$$w_k = \operatorname{int}\left(\frac{h_2 - h_s}{G_{sr}}\right), \tag{12}$$

where: $h_s = \sum_{i=1}^{i=8}\left[G_i \cdot \operatorname{int}\left(\frac{h_2 \cdot P_i}{G_i}\right)\right]$.

While total number of layers in a given fraction w_c, filled losslessly by microparticles, is defined by equation (13):

$$w_c = w_k + w_s, \tag{13}$$

where: $w_s = \sum_{i=1}^{i=8}\left[\operatorname{int}\left(\frac{h_2 \cdot P_i}{G_i}\right)\right]$,

w_s — number of layers completely filled with microparticles, according to symmetrical standard size distribution of these microparticles in the analysed fraction.

On this basis, for cylindrical test containers, the total amount of microparticles filling a given fraction n_c is defined by equation (14):

$$n_c = \sum_{i=1}^{i=w_s}\left[n_{ko}\left(R = R_i\right)\right] + \sum_{i=1}^{i=w_k}\left[n_{ko}\left(R = R_{sr}\right)\right], \tag{14}$$

where: $n_{ko}(R)$ — number of microparticles in a single layer of a cylindrical measurement container, consistent with their symmetrical normal distribution, in a given fraction — equation (8).

Similarly, the total volume of microparticles of different sizes in the analysed fraction is defined by equation (15):

$$V_{ce} = \sum_{i=1}^{i=w_s} \left[V_e \left(R = R_i \right) \cdot n_{ko} \left(R = R_i \right) \right] + \sum_{i=1}^{i=w_k} \left[V_e \left(R = R_{sr} \right) \cdot n_{ko} \left(R = R_{sr} \right) \right] \quad (15)$$

If the filling level for the whole fraction s_w is known and if the mass density for the whole fraction ρ_2 and for the base fluid ρ_o are known [22], it is possible to estimate the mean or averaged mass density of microparticles ρ_e according to equation (16):

$$\rho_e = \frac{\rho_2 - \rho_o \cdot \left(s_w - 1 \right)}{s_w} \quad (16)$$

It should be stressed that equation (16) only applies to cases where microparticle mass density does not depend on their size. Therefore, equation (16) only enables us to state that the estimation accuracy of the mass density of the studied microparticles (exemplified here by erythrocytes) depends mainly on the accuracy of determining the analysed fraction filling level s_w, and thus on the accuracy of microscopic measurements of microparticle size and their distribution throughout the fraction. Consequently, when biological microparticle mass is proportional to their volume, and indirectly to microparticle base dimensions, the proposed method of mass density estimation enables determining its value in relation to every layer that is completely filled with such microparticles. In this case, the level of a single layer filling with microparticles s_{wi} in a cylindrical measurement container is defined by equation (17):

$$s_{wi} = \frac{V_{ei} \cdot n_{ko} \left(R = R_i \right)}{F_p \cdot G_i}, \quad (17)$$

where: i — index of an individual layer, as used in the symbols in Table no. 1.

On account of the above, similarly to equation (16), microparticle mass density for each layer (or group of layers) can be estimated using equation (18):

$$\rho_{ei} = \frac{\rho_2 - \rho_o \cdot \left(s_{wi} - 1 \right)}{s_{wi}}. \quad (18)$$

In the presented method of estimating microparticle amount and mass density in fractions formed by centrifugal fractionation, the estimation accuracy depends strictly on the accuracy of representation of size and amount distribution of these microparticles in the fraction analysed.

5. Calculation examples

In the following examples, which verify the assumptions made for the method of approximate estimation of microparticle amount and mass density in complex biological mixtures using a fractionation process in a centrifugal force field, presented in this paper, the following literature data [37-40] were used:

a) as calculation input data:
   - erythrocyte fraction mass density: $\rho_2 = 1.095$ g/cm^3;
   - base fluid (plasma) mass density: $\rho_o = 1{,}025$ g/cm^3;
   - measurement container diameter ($D = 2{\cdot}R_{ko}$): $D = 8$ mm;
   - base side dimension of a square measurement container: $a_{kw} = 2{\cdot}R_{ko}$;
   - standard fraction values in a boundary equilibrium state following a centrifugal fractionation process (Fig. 1): $H = h_0 + h_1 + h_2$;
   - height of the analysed erythrocyte fraction (Fig. 1): $h_2 = 5$ mm;

b) for comparison as normative data:
   - erythrocyte amount in peripheral blood: $n_n = (4.2 – 6.2)$ million pcs./mm^3;
   - single erythrocyte cell volume: $V_{en} = (80\text{-}100)$ μm^3;
   - erythrocyte mass: $m_e = (27\text{-}346)$ pg;
   - erythrocyte base dimensions (as per Fig. 2): diameter (4-8.5) μm, thickness (1-3.5) μm, constriction (0.8-1.5) μm;

c) while for comparative calculations, the following data were assumed:
   - minimum and maximum diameter of erythrocytes observed in the analysed fraction: 7.8 μm and 8.5 μm;
   - erythrocyte thickness (Fig. 2): $G = 2{\cdot}R/4$;
   - erythrocyte constriction thickness (Fig. 2): $e = G/2$;
   - symmetrical normal distribution of microparticle size in the analysed sample with a standard deviation $\delta = 0.1$, consistent with the 3σ principle.

Calculation results are summarised in Tables 2 and 3 using similar symbols as in Table 1. Table 2 contains results of amount and mass density calculations for the studied microparticles for a sample symmetric normal distribution of their size. Table 3 in turn contains selected results from comparative calculations for a mixture filled losslessly in its entire volume with identical microparticles, using different measurement containers. In Table 2, microparticle radii R_i are mean values from the sub-ranges determined by standard deviation δ of a symmetrical normal deviation.

Table 2

Calculation results for the erythrocyte fraction using the presented method of estimating the amount and mass density for a symmetrical normal distribution and a cylindrical measurement container

i	$2{\cdot}R_i$ [μm]	V_{ei} [μm^3]	$n_{koi}(R = R_i)$	s_{wi}	ρ_{ei} [g/cm^3]	m_{ei} [pg]	n_i [million/mm^3]
1.	7.8	83.1257	937490	0.7951	1.6415	136.4500	9.56
2.	7.9	86.3640	911900	0.7933	1.6473	142.2717	9.19
3.	8.0	89.6854	890050	0.7940	1.6449	147.5269	8.85
4.	8.1	93.0908	869830	0.7955	1.6399	152.6637	8.55
5.	8.2	96.5813	848500	0.7953	1.6407	158.4639	8.23
6.	8.3	10.1580	827430	0.7946	1.6431	164.5741	7.93
7.	8.4	103.8220	806620	0.7934	1.6472	171.0151	7.64
8.	8.5	107.5743	790570	0.7962	1.6377	176.1713	7.40
	$2{\cdot}R_{sri}$ = 8.2	V_{esri} = 95.0502	$sum(n_{koi})$ = 6882390	s_{wsri} = 0.7947	ρ_{esri} = 1.6428	m_{esri} = 156.1420.	n_{sri} = 8.42

Symbols: i — layer index in a symmetrical normal distribution with standard deviation δ = 0.1 consistent with the 3σ principle (Table 1); R_i — current microparticle radius; R_{sri} — mean value of multiple layers; V_{ei} — volume of a single microparticle with radius R_i — equation 1; V_{esri} — mean microparticle volume in multiple layers; n_{koi} — amount of microparticles in a single layer — equation 8; s_{wi} — single layer level of filling with microparticles — equation 17; s_{wsri} — mean value of microparticle filling level from multiple layers; ρ_{ei} — microparticle mass density in layers; ρ_{esri} — mean value of microparticle mass density from multiple layers; m_{ei} — mass of a single microparticle in a given layer; m_{esri} — mean microparticle mass in the analysed fraction; n_i — number of microparticles of identical volume in 1 mm^3 of a given layer; n_{sri} — mean number of microparticles of identical volume from multiple layers in 1 mm^3 of a given fraction.

In Table 2, the mean values of the calculated parameters concern all fraction layers of the discussed symmetrical normal distribution. The mean values shown in Table 3 refer to the entire fraction comprising 2440 layers filled with microparticles of a constant radius R_{sr} = 4.1 μm and volume V_{esr} = 96.6 μm^3.

Table 3

Selected calculation results for erythrocytes of constant radius R_{sr} = 4.1 μm and volume V_{esr} = 96.6 μm^3 using different measurement containers

Shale of measurement container base	n	s_{wsr}	ρ_{esr} [g/cm^3]	m_{esr} [pg]	n_{sr} [million/mm^3]
Square	n_{kw} = 951810	0.7070	2.0007	193.2293	7.25
Hexagon	n_{sz} = 712970	0.8080	1.5986	154.3954	8.37
Circle	$n_{kosr}(R = R_{sr})$ = 848500	0.7953	1.6407	158.4639	8.23

Symbols: n — number of microparticles in a single layer, depending on the shape of the measurement container's base; n_{kw} — equation 6; n_{sz} — equation 7; $n_{kosr}(R = R_{sr})$ — equation 8; s_{wsr} — equation 17; ρ_{esr} — mean value of microparticle mass density, equation 18; n_{sr} — equation 14; m_{esr} — mean value of single microparticle mass in the analysed fraction.

6. Summary

In the presented method of estimating microparticle amount and mass using a process of fractionation of complex biological mixtures in a centrifugal force field, the accuracy is decided by the size distribution of these microparticles, determined through microscopic tests, with the assumption that mass density of the biological microparticles does not depend on their size, shape or development stage. This method, based on theoretical assumptions of an approximate erythrocyte model (Fig. 2), assumes that the analysed fraction and its individual layers are losslessly (as shown in Fig. 3) filled with microparticles in a state of boundary equilibrium, formed through a process of fractionation in a centrifugal force field [22]. The assumptions above, in particular the model of lossless and ordered filling of the analysed fraction, constitutes the basis of the fraction model described. An assessment of the accuracy of representation in this model of the actual fraction state is beyond the scope of this paper. Consequently, the numerical data determined using this model are estimates and only apply to a boundary equilibrium state formed in a process of rotational fractionation in a centrifugal force field [22].

Regardless of the limitations noted, the data can be used to formulate the following basic conclusions:

1. The accuracy of estimating the amount and mass density of microparticles in a given fraction mainly depends on the level of filling of individual layers with microparticles of specific size.
2. The accuracy of estimating the amount and mass density of microparticles in the analysed fraction markedly depends on the accuracy of representation of actual microparticle shape — Tables 2 and 3.
3. Compared to data from the literature [23-26], the geometric microparticle (erythrocyte) shape model proposed in the discussed method represents the microparticle volume fairly well despite the simplifications made to microparticle thickness G and constriction e (Fig. 2) — Table 2.
4. For microparticles arranged as in Fig. 3, a hexagonal and circular shape of the measurement container base provides the highest level of filling in the given fraction. Consequently, it is predicted that analyses performed using such containers will be the most accurate — Table 3. Calibrated containers with a hexagonal base are preferred for automated dynamic counting of microparticles [13-16]. On the other hand, containers with circular bases, due to the most common shape of blood sampling containers, will be preferred in standard preventive healthcare examinations.
5. For a symmetrical normal distribution of these values, estimation of the amount and size of microparticles in the analysed fraction using microscopic examinations can be limited to mean values from these tests — highlighted

lines in Tables 2 and 3. For other distributions, the analysis should be conducted similarly to the normal distribution presented herein.

6. Due to the assumption of lossless filling of individual fraction layers, the presented method of estimating the microparticle amount in the analysed fraction carries a certain error relative to literature data — Tables 2 and 3. Under actual conditions, this error is caused by other, even lighter microparticles trapped in a given fraction — both as a result of an incorrectly performed centrifugal fractionation process, and as a consequence of heterogeneity of the base fluid (plasma).
7. In the estimation method presented, when a statistical analysis of microparticle distributions in the analysed fraction is performed using automated microscopic methods [30, 33, 34], it is possible to greatly reduce the estimation error relative to previously used methods of sequential microparticle counting in the limited field of view of the measurement microscope.

It bears stressing that the most accurate estimation of microparticle amount and mass distribution is reached for binary biological mixtures. Nevertheless, in preventive morphological blood tests, the method presented can be successfully used for preliminary assessment of the patient's health, mainly due to the high repeatability of measurements. The main advantage of this method is its simplicity, speed and unambiguity of determination of the basic parameters that are directly related to normative parameters of blood. The method is easy to automate, and if comparable conditions of microscopic testing are maintained, also possible to perform using different measurement instruments. It is therefore a method that can be commonly used in medical laboratory tests as well as in testing of population patterns in peripheral blood.

Research funding source: author's own funds.

Received May 15, 2019. Revised June 28, 2019.

Andrzej Górka https://orcid.org/0000-0002-4690-4115

Paper translated into English and verified by company SKRIVANEK sp. z o.o., 22 Solec Street, 00-410 Warsaw, Poland.

REFERENCES

[1] Brettler D.B., Levine P., *Factor concentrates for treatment of hemophilia: Which one to choose?*, Blood, vol. 73, no. 8, 1989, 2067-2073, www.bloodjournal.org.

[2] Nishiyama K., Okudera T., Watanabe T. et al., *Basic characteristics of plazma rich in growth factors (PRGF): blood cell components and biological effects*, Clinical and Experimental Dental Research, John Wiley & Sons Ltd., 2016, www.ncbi.nlm.nih.gov/pmc/articles/PMC5839250/.

[3] *Lymphocyte Separation Medium for Isolation of Peripheral Blood Mononuclear Cells*, MP BiomedicalsEurope, 2018, www.mpbio.com.

[4] Konopka M., Kowalski Z., Fela K., Klamecka A., Cholewa J., *Otrzymywanie plazmy metodą wirowania krwi – charakterystyka procesu*, Wydawnictwo Politechniki Krakowskiej, Czasopismo Techniczne: Chemia, R.104, 1-Ch, 2007, 67-74, https://suw.biblos.pl.edu.pl.

[5] Rosiek A., *Hemafereza lecznicza i inne wybrane zagadnienia*, Journal of Transfusion Medicine, 5, 3, 2012, 140-145, www.fce.viamedica.pl.

[6] *Wytyczne w zakresie leczenia krwią i jej składnikami oraz produktami krwiopochodnymi w podmiotach leczniczych*, (praca zbiorowa), Publikacja sfinansowana przez ministra zdrowia w ramach programu: *Zapewnienie samowystarczalności Rzeczypospolitej Polskiej w zakresie krwi, jej składników i produktów krwiopochodnych*, Wojskowy Instytut Medyczny, Warszawa 2014, www.wim.mil.pl, Wyd. II, WEMA Wydawnictwo – Poligrafia Sp. z o.o., Warszawa 2014.

[7] Crocco I., Franchini M., Garozzo G., Gandini A.R., Gandini G., Bonomo P., Aprili G., *Adverse reactions in blood and apheresis donors: experience from two Italian transfusion centres*, Blood Transfus, 7, 1, 2009, 35-38, DOI 10.2450/2008.0018-08.

[8] Bialkowski W., Blank R.D., Zheng C., Gottschall J.L., Papanek P.E., *Impact of frequent apheresis blood donation on bone density: A prospective, longitudinal, randomized, controlled trial*, Bone Reports, 10, 2019, DOI: 10.1016/j.bonr.2018.100188, www.elsevier.com/locate/bonr.

[9] Infanti L., *Red cell apheresis: pros and cons*, International Society of Blood Transfusion, ISBT Science Series, 13, 2018, 16-22, DOI: 10.1111/voxs. 12397, https://onlinelibrary.wiley.com.

[10] Piao L., Park H., Hyunchul Jo Ch., *Theoretical prediction and validation of cell recovery rates in preparing platelet-rich plasma through a centrifugation*, Plos One, November 2, 2017, https://doi.org/10.1371/journal.pone.0187509.

[11] Hajjawi O.S., *Human red blood cells-1*, American Journal Life Sciences, 1, 5, 2013, 195-214, www.sciencepublishinggroup.com/j/ajls.

[12] Schallmoser K., Strunk D., *Preparation of pooled human platelet Lysate (pHPL) as an efficient supplement for animal serum-free human stem cell cultures*, PubMed, Journal of Visualized Experiments, October 2009, www.researchgate.net.

[13] Drela N., *Wprowadzenie do cytometrii przepływowej: metody znakowania komórek*, Zakład Immunologii WB UW, 2018, www.biol.uw.edu.pl.

[14] *Cytometria przepływowa BD*, BD Bioscience, 2018, www.biotechnologia.pl, www.bdbiosciences.co.eu.

[15] Sędek Ł., Sonsala A., Szczepański T., Mazur B., *Techniczne aspekty cytometrii przepływowej*, Journal of Laboratory Diagnostic, 46, 4, 2010, 415-420.

[16] *Cytometria przepływowa BD*, BD Bioscience 2018, www.biotechnologia.pl, www.bdbiosciences.co.eu.

[17] *Particle Separation*, Beckman Coulter Life Sciences, 2018, www.beckman.com.

[18] Oliva L., Baron C., Fernandez-Lopez J.A., Remesar X., Alemany M., *Marked increase in rat red blood cell membrane protein glycosylation by one-month treatment with a cafeteria diet*, 2015, DOI 10.7717/peerJ.1101, www.peerj.com.

[19] *Izolacja oraz analiza wybranych parametrów płytek krwi, cz. 2*, Innowacje Nauka Technologie, 2018, www.laboratorium.net.

[20] Norouzi N., Bhakta H.C., Grover W.H., *Sorting cells by their density*, PLOS One, vol. 12, 7, 2017.

[21] Górka A., *Viscosity and surface tension in the biological microparticle filtration process*, Biuletyn WAT, vol. 67, nr 1, 2018, 15-31, DOI: 10.5604/01.3001.0011.8015, www.biuletynwat.pl.

[22] Górka A., *Frakcjonowanie mikrocząstek biologicznych w polu grawitacji i polu sił odśrodkowych*, Biuletyn WAT, vol. 68, nr 1, 2019, 153-164 , DOI: 10.5604/01.3001.0013.1477, www.biuletynwat.pl.

[23] Tomaiuolo G., *Biomechanical properties of red blood cells in health and disease towards microfluidics*, Biomicrofluidics, 8, 051501, 2014, http://dx.doi.org/10.1063/1.4895755.

[24] Higgins J.M., Mahadevan L., *Physiological and pathological population dynamics of circulation human red blood cells*, PNAS, vol. 107, no. 47, 2010, 20587-20592, www.pnas.org/cgi/doi/10.1073/pnas.1012747107.

[25] Horbachevsky I.Ya., *Physiology of red blood cells, erythron, respiratory pigments, rheological properties of blood*, Termopil National Medical University, 2018, https://moodle.tdmu.edu.ua

[26] *Badanie krwi*, www.eduteka.pl © 2017.

[27] Guckenberger A., Kihm A., John T., Wagner C., Gekle S., *Numerical – experimental observation of shape bistability of red blood cells flowing in a microchannel*, 19 Nov. 2017, www.physics.bio-ph.com.

[28] Munoz S., Sebastian J.L., Sancho M., Alvarez G., *Modeling human erythrocyte shape and size abnormalities*, Cornell University, 2015, www.arxiv.org.

[29] Kim J., Lee H.Y., Shin S., *Advances in the measurement of red blood cells deformability: A brief review*, Journal of Cellular Biotechnology, 1, 2015, 63-79.

[30] Ustinov V.D., *On inverse reconstruction problems of erythrocyte size distribution in laser diffractometry*, Matem. Mod., vol. 29, no. 3, 2017, 51-62.

[31] *Pappus's centroid theorem*, 2018, https://en.wikipedia.org.

[32] Etcheverry S., Gallardo M.J., Solano P., Suwalsky M., Mesquita O.N., Saavedra C., *Real-time study of shape and thermal fluctuations in the echinocyte transformation of human erythrocytes using defocusing micoroscopy*, Journal of Biomedical Optics, 12, 28, 2018, www.spiedigitallibrary.org.

[33] Vuca P.V., Kikinda, *Determining the diameter of erythrocyte by means of manual laser*, IOSR Journal of Applied Physics (IOSR-JAP), vol. 6, iss. 3, ver. I, 2014, www.iosrjournals.org.

[34] Wriedt T., Hellmers J., Eremina E., Schuh R., *Light scattering by single erythrocyte: Comparison of different methods*, Journal of Quantitative Spectroscopy & Radiative Transfer, 100, 2006, 441-456, www.elsevier.com.

[35] *Cassini oval*, 2018, www.wikipedia.org

[36] Karatas M., *A multi foci closed curve: Cassini oval, its properties and applications*, Dogus Universitesi Dergisi, 14, 2, 2013, 231-248, www.nps.edu.

[37] Trudnowski R.J., Rico R.C., *Specific gravity of blood and plasma at 4 and 37°C*, Clinical Chemistry, vol. 20, no. 5, 1974, 615-616.

[38] Reznikoff P., *A method for the determination of the specific gravity of blood cells*, Journal of Experimental Medicine, 38, 4, 1923 Sep. 30, 441-445.

[39] *Density of Blood*, The Physics Factbook 2018, https://hypertextbook.com/act/2004/MichaelShmukler.shtml

[40] Diez-Siva M., Dao M., Han J., Lim Ch-T., Suresh S., *Shape and biomechanical characteristics of human red blood cells in health and disease*, HHS Public Access MRS Bull., 35, 5, 2010 May 382-388, www.ncbi.nlm.nih.gov/pmc/.

A. GÓRKA

Metoda przybliżonego wyznaczania ilości i masy mikrocząstek w mieszaninach biologicznych z zastosowaniem procesu frakcjonowania w polu sił odśrodkowych

Streszczenie. W publikacji przedstawiono uproszczoną metodę szacowania ilości i masy właściwej mikrocząstek w złożonych mieszaninach biologicznych z zastosowaniem procesu frakcjonowania w polu sił odśrodkowych. W prezentowanej metodzie, na przykładzie najcięższych komórek krwi erytrocytów, wykorzystano geometryczny model binarnej frakcji w stanie granicznej równowagi, uformowanej w procesie frakcjonowania krwi. W modelu tym zastosowano opracowany aproksymacyjny kształt erytrocytu oraz przykładowy rozkład normalny wielkości i ilości mikrocząstek w badanej modelowej frakcji. Na podstawie ogólnie dostępnych danych dotyczących krwi wykazano, że przedstawiona metoda umożliwia oszacowanie ilości i masy właściwej mikrocząstek w polu sił odśrodkowych. Dokładność takiego szacowania generalnie zależy od precyzji odwzorowania kształtów, stopnia wypełnienia frakcji mikrocząsteczkami oraz od indywidualnego rozkładu ilościowego i wymiarowego tych cząstek w badanej frakcji. Powyższe wnioski, stanowiące o dokładności prezentowanej metody, w publikacji zweryfikowano z wykorzystaniem ogólnie dostępnych w literaturze danych reologicznych krwi. Jednocześnie na podstawie uzyskanych wyników obliczeniowych wykazano wpływ kształtu pojemników pomiarowych na stopień wypełnienia danej frakcji mikrocząsteczkami.

Słowa kluczowe: frakcjonowanie mieszanin biologicznych, frakcjonowanie składników krwi, model erytrocytu, kształt erytrocytu, składniki krwi

DOI: 10.5604/01.3001.0013.5552